Atypical Thermonuclear Supernovae from Tidally Crushed White Dwarfs

Stephan Rosswog[1], Enrico Ramirez-Ruiz[2], and William R. Hix[3]

ABSTRACT

Suggestive evidence has accumulated that intermediate mass black holes (IMBHs) exist in some globular clusters. As stars diffuse in the cluster, some will inevitable wander sufficiently close to the hole that they suffer tidal disruption. An attractive feature of the IMBH hypothesis is its potential to disrupt not only solar-type stars but also compact white dwarf stars. Attention is given to the fate of white dwarfs that approach the hole close enough to be disrupted and compressed to such extent that explosive nuclear burning may be triggered. Precise modeling of the dynamics of the encounter coupled with a nuclear network allow for a realistic determination of the explosive energy release, and it is argued that ignition is a natural outcome for white dwarfs of all varieties passing well within the tidal radius. Although event rates are estimated to be significantly less than the rate of normal Type Ia supernovae, such encounters may be frequent enough in globular clusters harboring an IMBH to warrant a search for this new class of supernova.

Subject headings: black hole physics – supernova: general – white dwarfs – globular clusters: general

1. Introduction

The conjecture that there may be an intermediate mass black hole (IMBH) in some globular clusters has gained credence over the past few years. There is some dynamical evidence for a mass concentration within the central regions of some globular clusters. In particular,

[1]School of Engineering and Science, Jacobs University Bremen, Campus Ring 1, 28759 Bremen, Germany; s.rosswog@jacobs-university.de

[2]Department of Astronomy and Astrophysics, University of California, Santa Cruz, CA 95064; enrico@ucolick.org

[3]Physics Division, Oak Ridge National Laboratory, Oak Ridge, TN37831-6374; raph@phy.ornl.gov

the dynamics of stars in the inner regions of nearby clusters such as M15 and G1 suggest the presence of black holes with masses of the order of 10^3 and 10^4 $M_\odot$, respectively (Gerssen et al. 2002, 2003; Gebhardt et al. 2002, 2005). This evidence remains rather controversial, partly because the velocity dispersion profiles can be reproduced without invoking the presence of an IMBH. Recently, somewhat more ambiguous evidence has arisen for the presence of IMBHs in young star clusters, where ultraluminous, compact X-ray sources (ULXs) have been preferentially found to occur (Zezas et al. 2002; Pooley & Rappaport 2006). Their high luminosities suggest that they are IMBHs rather than binaries containing a normal stellar mass black hole. Studies based on detailed N-body simulations (Portegies Zwart et al. 2004; Patruno et al. 2006) of the evolution of a young star cluster in M82, the position of which coincides with an ULX, give further credence to this idea. While none of these arguments in itself carries enough weight to be convincing, the fact that they are so different in character does suggest that the existence of IMBHs in some young star clusters should be taken seriously.

One would like some independent corroboration of the IMBH hypothesis, or, conversely, some way of ruling it out. Stellar disruption potentially offers such a test. As stellar orbits diffuse in phase space, it therefore seems inevitable that some will wander sufficiently close to the hole that they suffer tidal disruption. A star interacting with a massive black hole cannot be treated as a point mass if it gets so close to the hole that it becomes vulnerable to tidal deformations (Frank & Rees 1976). The tidal radius, $r_{\rm T}$, defined as the distance within which a stars gets tidally disrupted, obviously has a value that depends on the type of star being considered. For a solar-type star it is

$$r_{\rm T} = \left(\frac{M_{\rm h}}{M_\odot}\right)^{1/3} r_\odot \simeq 5\times 10^{12} M_{\rm h,6}^{1/3} r_\odot M_\odot^{-1/3}\ {\rm cm}, \tag{1}$$

while for a degenerate white dwarf is roughly

$$r_{\rm T} \simeq 10^{11} M_{\rm h,6}^{1/3} r_{\rm wd,9} M_{\rm wd,0.6}^{-1/3}\ {\rm cm}. \tag{2}$$

Here $r_{\rm wd,9}$ and $M_{\rm wd,0.6}$ denote the white dwarf radius and mass in units of 10^9 cm and $0.6M_\odot$, respectively. Note that for white dwarfs, the tidal radius is indeed inside the gravitational radius, $r_{\rm g} \simeq 1.5\times 10^{11} M_{\rm h,6}$ cm, for black holes masses exceeding

$$M_{\rm h,lim} \sim 10^5 r_{\rm wd,9}^{3/2} M_{\rm wd,0.6}^{-1/2}\ M_\odot. \tag{3}$$

For this reason, tidal disruption of white dwarfs offers a unique diagnostic for the presence of an IMBH (Luminet & Pichon 1989; Wilson & Mathews 2004; Baumgardt et al. 2004). This paper explores the observational manifestations of such phenomena, with particular reference to white dwarfs that approach the hole close enough to be disrupted and severely compressed.

2. Numerical Methods

The observational consequences of stellar disruption depend on what happens to the debris (Rees 1998; Evans & Kochanek 1989). To quantify this, we have performed detailed three-dimensional, hydrodynamical calculations. The gas dynamics is coupled with a nuclear network to explore the effects of explosive nucleosynthesis during the strong compression phase.

Hydrodynamics. The smoothed particle hydrodynamics method (SPH) is used here to solve the equations of hydrodynamics. Due to its Lagrangian nature SPH is perfectly suited to follow tidal disruption processes during which the corresponding geometry, densities and time scales are changing violently. The SPH-formulation used in this study follows closely the one described in Benz (1990). The SPH equations derived from a Lagrangian (Springel & Hernquist 2002; Monaghan 2002) yield different symmetries in the particle indices, but a recent comparison (Rosswog & Price 2007) between these two sets of equations found only very minor differences. The forces from self-gravity are evaluated via a binary tree (Benz et al. 1990b), the gravitational forces from the central black hole are calculated using a Paczyński-Wiita pseudo potential (Paczyński & Wiita 1980). Details of how the singularity is treated numerically can be found in Rosswog (2005). We have taken particular care to avoid artifacts from the use of artificial viscosity (AV). The so-called Balsara-switch (Balsara 1995) is implemented here to avoid spurious shear forces. In addition, time-dependent viscosity parameters (Morris & Monaghan 1997) are used so that AV is only present where really needed. Details of the AV implementation and tests can be found in Rosswog et al. (2000).

Equation of state. The HELMHOLTZ equation of state (EOS), developed by the Center for Astrophysical Thermonuclear Flashes at the University of Chicago is used. This EOS accepts an externally calculated chemical composition, facilitating the coupling to nuclear reaction networks. The electron-/positron equation of state makes no assumptions about the degree of degeneracy or relativity and the exact expressions are integrated numerically and tabulated. The interpolation in this table enforces thermodynamic consistency by construction (Timmes & Swesty 2000). The nuclei in the gas are treated as a Maxwell-Boltzmann gas, the photons as blackbody radiation.

Nuclear burning. To account for the feedback onto the fluid from nuclear transmutations we use a minimal nuclear reaction network developed by Hix et al. (1998). It couples a conventional α-network stretching from He to Si with a quasi-equilibrium-reduced α-network for temperatures in excess of $3 \cdot 10^9$ K. Although a set of only seven nuclear species is used, this network reproduces all burning stages from He-burning to nuclear statistical equilibrium (NSE) accurately. For details and tests we refer to Hix et al. (1998).

3. Tidal Crushing and Ignition of White Dwarfs

Several snapshots taken from our numerical simulations of a 0.2 $M_\odot$ white dwarf approaching a $10^3 M_\odot$ black hole on a parabolic orbit with pericenter distance well within the tidal radius ($r_{\rm min} = r_{\rm T}/12$) are shown in Figure 1. While falling inwards towards the hole, the star develops a quadrupole distortion which attains an amplitude of order unity by the time of disruption at $r \sim r_{\rm T}$. The resultant gravitational torque spins it up to a good fraction of its corotation angular velocity by the time it gets disrupted. The large surface velocities and the order unity tidal bulge combine to overcome the star's self gravity and lead to the disruption of the star.

The behavior of a white dwarf passing well within the tidal radius exhibits special features (Luminet & Pichon 1989). As illustrated in Figure 1, the degenerate star is not only elongated along the orbital direction but is even more severely compressed into a prolate shape (i.e., a pancake aligned in the orbital plane). Each section of the star is squeezed through a point of maximum compression at a fixed point on the star's orbit. During this very short lived phase, the pressure grows sharply and the matter is raised to a higher adiabat. The distortions $\Delta r_{\rm wd}/r_{\rm wd} \sim 1$ impart supersonic bulk flow velocities during the drastic compression of the stellar material. As a result, the temperatures increase sharply and trigger explosive burning (of He for the case shown in Figure 1). The corresponding energy release can be very large (more than the star's self gravity) and it can build up sufficient pressure to significantly modify the dynamical evolution. Figure 2 shows the evolution of the compressed, and tidally disrupted white dwarf with and without the effects of nuclear burning. The pressure cannot build up sufficiently until after the white dwarf has endured a substantial volume contraction. This contraction is halted further by nuclear energy release. Just after the white dwarf attains its maximum compression, the density drops dramatically as a result of the subsequent expansion.

During the brief but strong compression phase, the temperature reaches values beyond 3×10^9 K, approaching but not quite reaching NSE. As a result, nuclei up to and beyond silicon are synthesized from the initially pure ^{4}He 0.2 $M_\odot$ white dwarf. The initial composition was pure ^{4}He and the final mass fraction in iron-group nuclei is roughly 15%, located near the center (Figure 3). This result should be taken as a modest underestimate, due to limitations in the seven species nuclear reaction network. Post-processing calculations, using a 300 isotope nuclear network over thermodynamic histories resulting from these calculations, show significant nuclear flow above silicon, for helium- rich portions of the gas with peak temperatures above 2×10^9K. As a result, heavier elements (like calcium, titanium and chromium) would be made, accompanied by a modest increase in the energy generation. It is thus safe to conclude that the white dwarf is tidally ignited and that a sizable mass of

iron-group nuclei is injected into the flow. Although the thermodynamical evolution and the nuclear energy release are sensitive to the initial stellar composition, here assumed to be ^{4}He, we found that ignition is a natural outcome for white dwarfs of all masses (e.g. massive white dwarfs deprived of helium resulting from the evolution of a medium mass star) passing well within the tidal radius. For example, a C/O 0.6 $M_\odot$ (1.2 $M_\odot$) white dwarf approaching a 500 M black hole on a parabolic orbit with pericenter distance $r_{\rm min} = r_{\rm T}/5$ ($r_{\rm min} = r_{\rm T}/2.6$) ignites and, as a result, at least 0.17 (0.66) $M_\odot$ of iron-group nuclei are synthesized in the flow. Thus, in the most favorable cases, the nuclear energy release may be comparable to that of typical type Ia supernovae.

Although the explosion will increase the fraction of ejected debris, enough remains to be accreted on to the hole (Figure 4). The returning gas does not immediately produce a flare of activity from the black hole. First material must enter quasi circular orbits and form an accretion torus (Rees 1998; Evans & Kochanek 1989). Only then will viscous effects release enough binding energy to power a flare. The bound orbits are very eccentric, and the range of orbital periods is large. For white dwarfs, the orbital semi-major axis of the most tightly bound debris is $a \sim 300 M_{\rm h,3}^{-1/3} r_{\rm wd,9} M_{\rm wd,0.6}^{-2/3}\ r_{\rm g}$, and the period is only $t_{\rm a} \sim 150 (a/300 r_{\rm g})^{3/2} M_{\rm h,3}^{-1/2}$ s. The simulation shows that the first material returns at a time $\leq t_{\rm a}$, with an infall rate roughly given by $10^2 M_\odot$ yr^{-1}. Such high infall rates are expected to persist, relative steadily, for at least a few orbital periods, before all the highly bound material rains down. The vicinity of the hole would thereafter be fed solely by injection of the infalling matter at a rate that drops off roughly as $t^{-5/3}$ for $t \geq t_{\rm fb} \approx 600$ s. Once the torus is formed, it will evolve under the influence of viscosity, radiative cooling winds and time dependent mass inflow. A luminosity $\sim L_{\rm Edd} = 10^{41} M_{\rm h,3}$ erg s^{-1} can therefore only be maintained for at most a year; thereafter the flare would rapidly fade. It is clear that most of the debris would be fed to the hole far more rapidly than it could be accepted if the radiative efficiency were high; much of the bound debris must either escape in a radiatively-driven outflow or be swallowed inefficiently. The rise and the peak bolometric luminosity can be predicted with some confidence. However, the effective surface temperature (and thus the fraction of luminosity that emerges predominantly in the soft X-ray band) is harder to predict, as it depends on the size of the effective photosphere that shrouds the hole.

4. Discussion

Exactly how often a star gets close enough to the central hole to be tidally disrupted depends on the stellar velocity distribution in star clusters (Frank & Rees 1976). In a simple case when the velocities are isotropic, the frequency with which a star enters the zone of

vulnerability is

$$\sim 10^{-7} M_{\rm h,3}^{4/3} \left(\frac{n_*}{10^6\ {\rm pc}^{-3}}\right) \left(\frac{\sigma}{10\ {\rm km\ s}^{-1}}\right)^{-1} \left(\frac{r_{\rm min}}{r_{\rm T}}\right)\ {\rm yr}^{-1}, \tag{4}$$

where n_* is the star density in the star cluster nucleus and $M_{\rm h,3}$ is the hole's mass in units of $10^3 M_\odot$. This fiducial capture rate may need to be modified for a number of reasons. The actual rate could be lower than that given by equation (4), even if the initial distribution were isotropic, if the *loss cone* orbits were depleted faster than they could be replenished (Frank & Rees 1976). If the relaxation timescale were short enough to ensure replenishment of the loss cone, then the same diffusion processes could build up a *cusp* in the stellar distribution near the black hole. Capture or disruption of these stars could then augment the rate given by equation (4). None of these complications is, however, likely to seriously modify the simple estimate given above (Baumgardt et al. 2004). The rate given by equation (4), although highly simplified, agrees well with the fiducial rates derived from detailed $N-$body simulations of multimass star clusters containing IMBHs (Baumgardt et al. 2004). However, in these simulations Baumgardt and collaborators found that IMBHs in star clusters disrupt mainly main sequence stars and giants, with white dwarfs accounting for only a few tenths of all disruptions. The probability of a pericentric distance within $r_{\rm min}$ is proportional to the first power of $r_{\rm min}$ (see equation [4]). While complete disruption requires $r_{\rm min} \leq r_{\rm T}$, ignition, as calculated here, appears to be a natural outcome for white dwarfs passing well within the tidal radius: $r_{\rm min} \leq r_{\rm T}/\xi$ with $\xi \geq 3$. The actual rate for white dwarf ignition would then be at least an order of magnitude lower than that given by equation (4).

It may seem, however, that even the modest rate of stellar disruptions given in equation (4) could have conspicuous consequences. The mass fraction that is ejected rather than swallowed, though less spectacular than typical Ia supernovae (Hillebrandt & Niemeyer 2000), could nevertheless have distinctive observational signatures. The ejected material would be concentrated in a cone or *fan* close to the orbital plane (Figure 3). The characteristic velocities in excess of $\sim 2 \times 10^4$ km/s (Figure 3), the kinetic output when a white dwarf is disrupted being $\sim 4 \times 10^{50}$ erg s^{-1}. The light curve powered by radioactive decay, would indicate the synthesis of at least $0.1 M_{\rm wd}$ of ^{56}Ni before the spray of gas becomes translucent. With a rate of disruption of white dwarfs $\xi \sim 10^{-8}$ yr^{-1} per globular cluster (Baumgardt et al. 2004), we expect the mean time interval between successive captures per galaxy to be $\sim 10^5 (\xi/10^{-8}\ {\rm yr}^{-1})^{-1} (f_{\rm bh} N_{\rm gc}/10^3)^{-1}$ yr, where $f_{\rm bh} N_{\rm gc}$ is the average number of globular clusters harboring an IMBH per galaxy and the number of globular clusters per host, $N_{\rm gc}$, is found, for example, to vary between 5×10^2 and 7×10^3 from dwarf ellipticals to giant ellipticals (van den Bergh 1998; Brodie & Strader 2006). Event rates are then estimated to be significantly less than the rate of type Ia supernovae, which have an observed time interval between one type Ia explosion and the next of about 10^2 yr (Leibundgut 2001; Sharon

et al. 2007), but could be frequent enough to warrant a search for this new class of optical transient.

The transient sky at faint magnitudes is poorly known, but there are major efforts under way that would increase the discovery rate for type Ia supernovae from a few thousands (Aldering et al. 2007) to about hundreds of thousands (Riess & Livio 2006) per year. The transient itself should have several distinguishing characteristics. First, it should be seen in association with a globular cluster. Second, the explosion itself should be different, since the disrupted, degenerate stars should be, on average, lighter than those exploding as type Ia supernovae. Third, the spectra should exhibit large Doppler shifts, as the ejected debris would be expelled with speeds $\geq 10^4$ km/s and the optical light curve should be rather unique as a result of the radiating material being highly squeezed into the orbital plane (one thus expects different timescales for conversion of nuclear energy to observable luminosity when compared with normal type Ia events). Finally, the peculiar, underluminous thermonuclear explosion should be accompanied by a thermal transient (predominantly of soft X-ray emission) signal with peak intensity $L \sim L_{\rm Edd} = 10^{41} M_{h,3}$ erg/s, fading within a year. Such transient signals, if detected, would be a compelling testimony for the presence of IMBHs in the centers of globular clusters.

We thank Holger Baumgardt, Peter Goldreich, Jim Gunn, Piet Hut, Dan Kasen and Martin Rees for very useful discussions. The simulations presented in this paper were performed on the JUMP computer of the Höchstleistungsrechenzentrum Jülich. E. R. acknowledges support from the DOE Program for Scientific Discovery through Advanced Computing (SciDAC; DE-FC02-01ER41176). W. R. H. has been partly supported by the National Science Foundation under contracts PHY-0244783 and AST-0653376. Oak Ridge National Laboratory is managed by UT-Battelle, LLC, for the U.S. Department of Energy under contract DE-AC05-00OR22725.

REFERENCES

Aldering, G., et al. 2007, Astroparticle Physics, 27, 213

Balsara, D. S. 1995, J. Comp. Phys., 121, 357

Baumgardt, H., Makino, J., & Ebisuzaki, T. 2004, ApJ, 613, 1143

Benz, W. 1990, Numerical Modelling of Nonlinear Stellar Pulsations Problems and Prospects, 269

Benz, W., et al. 1990, ApJ, 348, 647

Brodie, J. P., & Strader, J. 2006, ARA&A, 44, 193

Evans, C. R., & Kochanek, C. S. 1989, ApJ, 346, L13

Frank, J., & Rees, M. J. 1976, MNRAS, 176 633

Gebhardt, K., Rich, R. M., & Ho, L. C. 2002, ApJ, 578 L41

Gebhardt, K., Rich, R. M., & Ho, L. C. 2005, ApJ, 634, 1093

Gerssen, J., et al. 2002, AJ, 124, 124, 3270

Gerssen, J., et al. 2003, AJ, 125, 376

Hillebrandt, W., & Niemeyer, J. C. 2000, ARA&A, 38, 191

Hix, W. R., et al. 1998, ApJ, 503, 332

Leibundgut, B. 2001, ARA&A, 39, 67

Luminet, J.-P., & Pichon, B. 1989, A&A, 209, 103

Monaghan, J.J. 2002, MNRAS 335, 843

Morris, J., & Monaghan, J. 1997, J. Comp. Phys., 136, 41

Paczyński, B., & Wiita, P. 1980, A&A, 88, 23

Patruno, A., et al. 2006, MNRAS, 370, L6

Pooley, D., & Rappaport, S. 2006, ApJ, 644, L45

Portegies Zwart, S. F., et al. 2004, Nature, 428, 724

Riess, A. G., & Livio, M. 2006, ApJ, 648, 884

Rees, M. J. 1988, Nature, 333, 523

Rosswog, S., et al. 2000, A&A, 360, 171

Rosswog, S. 2005, ApJ, 634, 1202

Rosswog, S. & Price. D.J. 2007, MNRAS, 379, 915

Sharon, K., et al. 2007, ApJ, 660, 1165

Springel, V. & Hernquist, L. 2002, MNRAS, 333, 649

Timmes, F. X. & Swesty, F. D. 2000, ApJS, 126, 501

van den Bergh, S. 1998, ApJ, 492, 41

Wilson, J. R., & Mathews, G. J. 2004, ApJ, 610, 368

Zezas, A., et al. 2002, ApJ, 577, 710

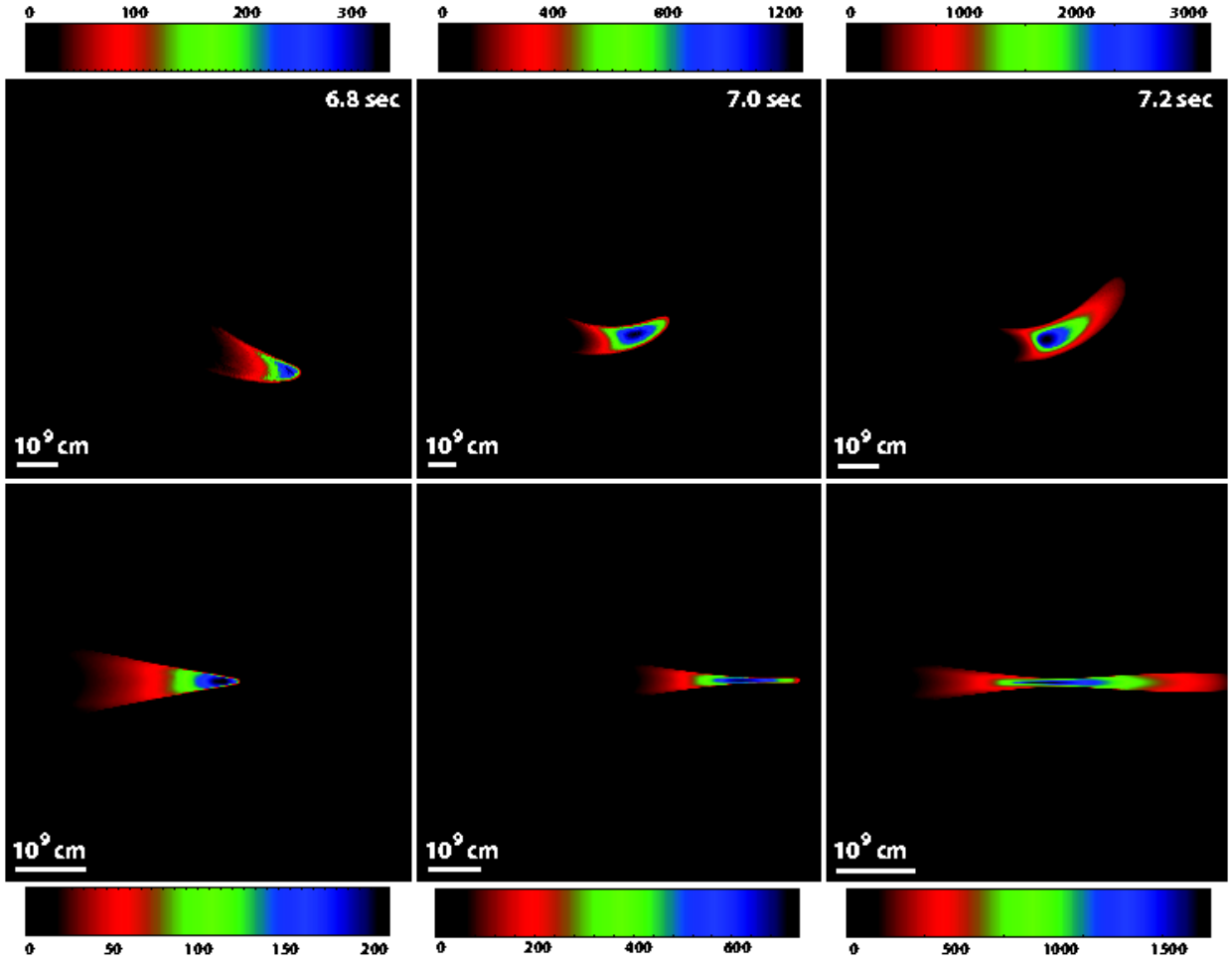

Fig. 1.— A 0.2 $M_\odot$ white dwarf (modeled with more than 4×10^6 SPH particles) approaching a 10^3 $M_\odot$ black hole on a parabolic orbit with pericenter distance $r_{\rm min} = r_{\rm T}/12$ is distorted, spun up during infall and then tidally disrupted. Temperatures (in units of 10^6 K) of the white dwarf-black hole encounter are shown. The panels in the upper row show cuts through the orbital (xy-) plane before and after passage through pericenter, as the white dwarf attains its maximum degree of compression. The panels in the lower row show the temperature distribution in the xz-pane (averaged along the y-direction).

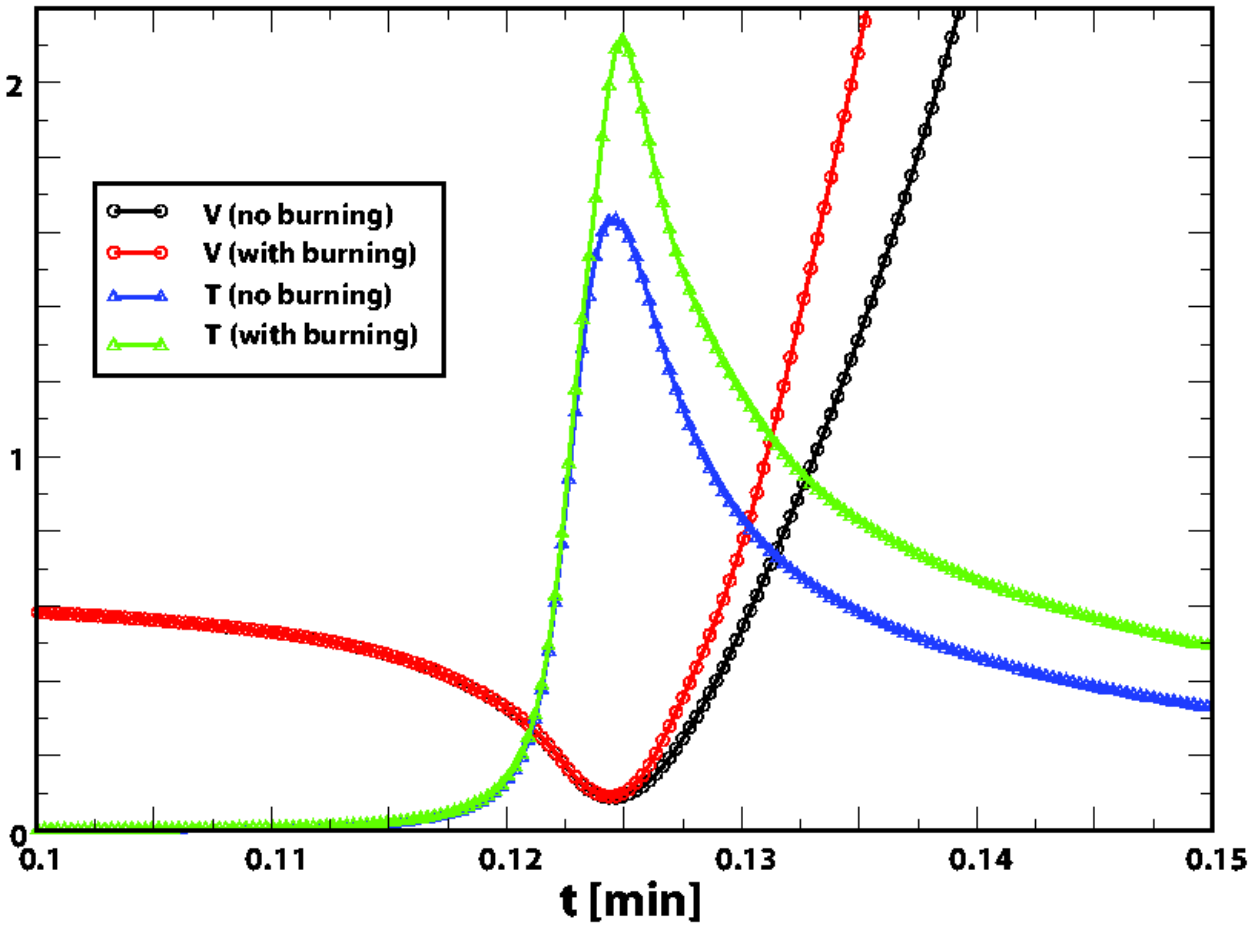

Fig. 2.— Evolution of the thermodynamical and mechanical properties of the central portion of the disrupted white dwarf. In this test calculation twenty central SPH-particles are chosen and their average temperature and volume ($V = \sum_i m_i/\rho_i$ with m_i particle mass and ρ_i particle density) evolution is followed during passage through pericenter. As the star penetrates deeply within the tidal radius, the pressure cannot build up sufficiently until after the star has undergone an important volume contraction. The strong compression of the volume goes along with a sharp temperature increase. When burning is taken into account (red and green curves), the pressure terms grows very sharply, and, as a result, the temperature (averaged over the chosen set of particles) increases beyond 2.1×10^9 K.

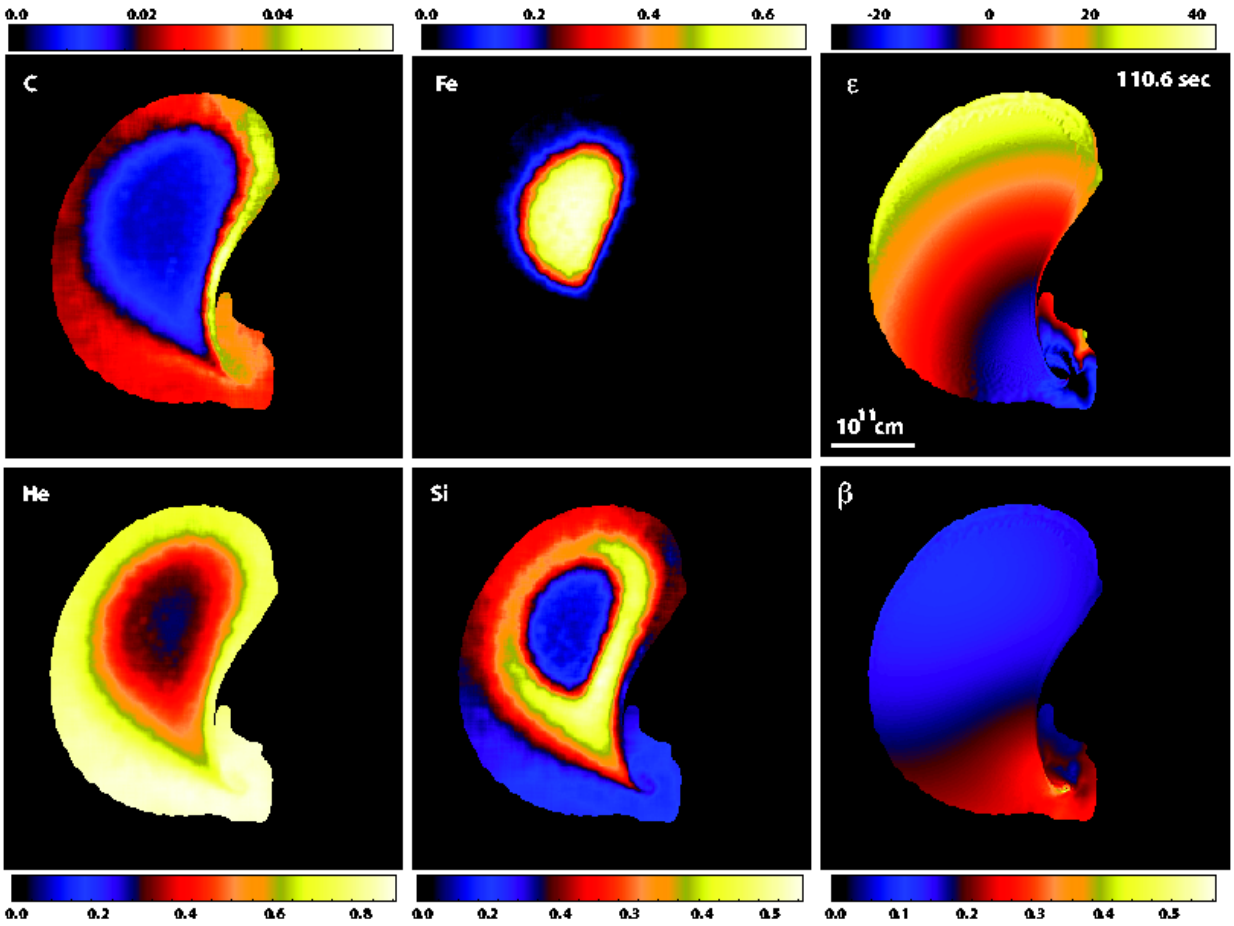

Fig. 3.— The nature of the unbound debris at 110.6s. The panels show cuts through the orbital (xy-) plane well after passage through pericenter. The panels in the left columns show the mass fraction distributions of the synthesized group elements. The panels in the right column show the velocity distribution, $\beta = v/c$, and the specific energy, ϵ, (in code units).

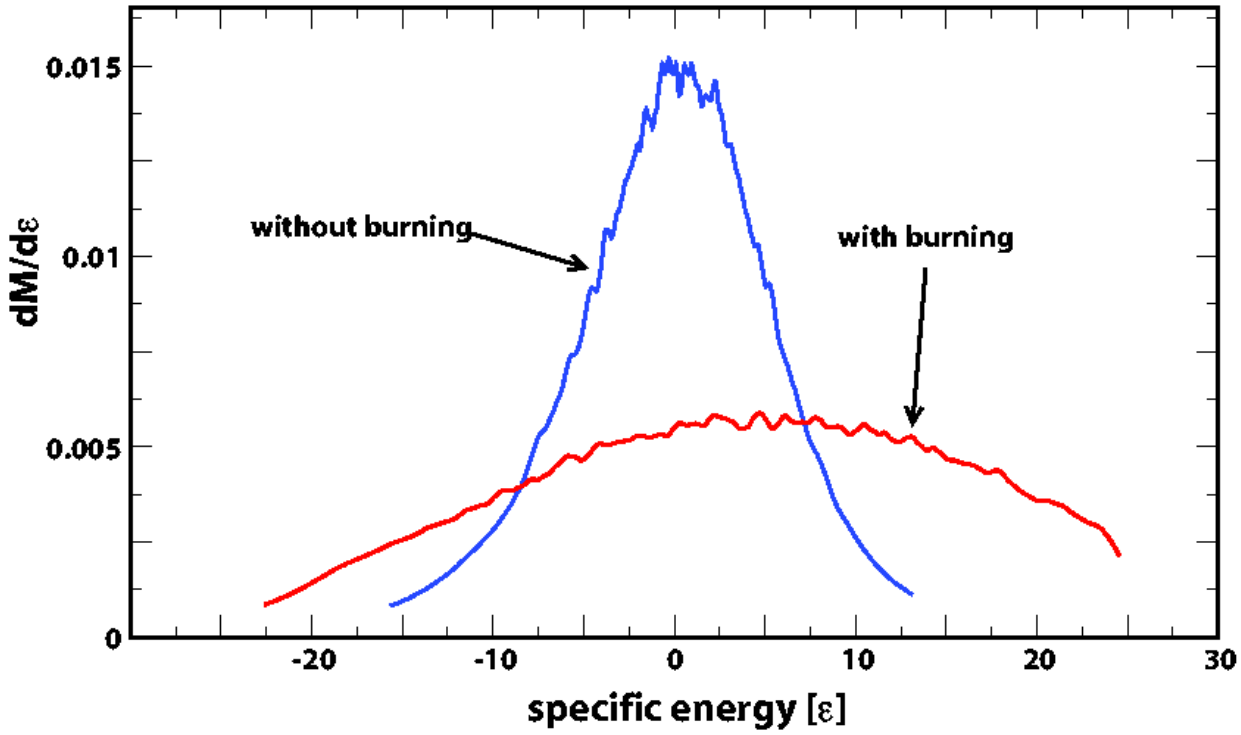

Fig. 4.— Influence of the nuclear burning on the ejected matter: differential mass distributions in specific energy for the 0.2 $M_{\odot}$ white dwarf debris. The resultant explosive energy severely decreases the amount of material bound to the hole from 50% to 35% of the initial mass of the white dwarf.